Regular Article

Accuracy of the non-relativistic approximation for momentum diffusion

Shiuan-Ni Liang and Boon Leong Lan[a]

Electrical and Computer Systems Engineering, School of Engineering, Monash University, 47500 Bandar Sunway, Malaysia

Abstract. The accuracy of the non-relativistic approximation, which is calculated using the same parameter and the same initial ensemble of trajectories, to relativistic momentum diffusion at low speed is studied numerically for a prototypical nonlinear Hamiltonian system –the periodically delta-kicked particle. We find that if the initial ensemble is a non-localized semi-uniform ensemble, the non-relativistic approximation to the relativistic mean square momentum displacement is always accurate. However, if the initial ensemble is a localized Gaussian, the non-relativistic approximation may not always be accurate and the approximation can break down rapidly.

Introduction

Low-speed momentum diffusion in nonlinear Hamiltonian systems has been studied [1–12] extensively using non-relativistic, Newtonian mechanics. The statistical quantity that is typically used to study momentum diffusion is the mean square momentum displacement (MSMD) [1–3,7,10,11]. In previous studies [1–3] of momentum diffusion in the Newtonian standard map for the periodically delta-kicked particle, an initially non-localized semi-uniform ensemble of trajectories (where semi-uniform means that the initial positions are uniformly distributed but the initial momenta are all the same value) was typically used in the numerical calculation of the MSMD. These studies [2,3] of the Newtonian standard map have shown that, for parameter K where accelerator mode islands (these are stable regions in the chaotic sea [13] in which the particle accelerates continuously [13,14]) exist, the MSMD has a power-law dependence on the kick n: n^α, where $1 < \alpha < 2$, *i.e.*, the diffusion is anomalous. In contrast, for parameter K where there is no accelerator mode island, the MSMD grows linearly [1–3], *i.e.*, the diffusion is normal. Considerable effort has been made recently to understand anomalous diffusion in nonlinear Hamiltonian systems —see, for example, the article by Altmann and Kantz [15] and the review by Zaslavsky [16].

Recently, Matrasulov *et al.* [17] studied both low-speed (weak-relativistic) and high-speed (ultra-relativistic) momentum diffusion in the special-relativistic standard map for the periodically delta-kicked particle. However, a comparison of the Newtonian and special-relativistic predictions for *low-speed* momentum diffusion has not yet been done to ascertain if the special-relativistic prediction is always well approximated by the Newtonian prediction as would be expected [18,19]. Such a comparison is important since Newtonian mechanics is the standard theory used in practice, instead of special-relativistic mechanics, to study low-speed momentum diffusion. In this paper, we compare the low-speed momentum diffusion predicted by the two theories, based on the same parameter and the same ensemble of initial conditions, for the periodically delta-kicked particle. In addition to the initially non-localized semi-uniform ensemble typically used in the Newtonian [1–3] and special-relativistic [17] calculations of momentum diffusion for the kicked particle, we also use an initially localized ensemble in our calculations for comparison. Details of the kicked particle and numerical calculations are given next, followed by the presentation and discussion of the results and conclusion.

Methods

The periodically delta-kicked particle is a one-dimensional Hamiltonian system where the delta kicks are due to a sinusoidal potential which is periodically turned on for an instant. The Newtonian equations of motion for the

---

[a] e-mail: lan.boon.leong@monash.edu

periodically delta-kicked particle are easily integrated [1,20] to yield an exact mapping, which is known as the standard map, of the dimensionless scaled position X and dimensionless scaled momentum P from just before the $(n-1)$-th kick to just before the n-th kick:

$$P_n = P_{n-1} - \frac{K}{2\pi} \sin(2\pi X_{n-1}) \tag{1}$$

$$X_n = (X_{n-1} + P_n) \mod 1, \tag{2}$$

where $n = 1, 2, \ldots$, and K is a dimensionless positive parameter. The transition from local to global chaos in phase space for the Newtonian standard map above occurs [21] at $K = 0.971635\ldots$. The special-relativistic equations of motion for the periodically delta-kicked particle are also easily integrated [22,23] to yield an exact mapping for the dimensionless scaled position X and dimensionless scaled momentum P from just before the $(n-1)$-th kick to just before the n-th kick:

$$P_n = P_{n-1} - \frac{K}{2\pi} \sin(2\pi X_{n-1}) \tag{3}$$

$$X_n = \left(X_{n-1} + \frac{P_n}{\sqrt{1 + \beta^2 P_n^2}} \right) \mod 1, \tag{4}$$

where $n = 1, 2, \ldots$. In addition to the parameter K, the relativistic standard map (eqs. (3) and (4)) has another dimensionless positive parameter, β. Since

$$\frac{v}{c} = \frac{\beta P}{\sqrt{1 + (\beta P)^2}}, \tag{5}$$

$\beta P \ll 1$ implies $v \ll c$ (*i.e.*, low speed), where v is the particle speed and c is the speed of light. At low speed, the relativistic standard map (eqs. (3) and (4)) is [24] approximately

$$P_n = P_{n-1} - \frac{K}{2\pi} \sin(2\pi X_{n-1}) \tag{6}$$

$$X_n = \left[X_{n-1} + \left(1 - \frac{1}{2} \beta^2 P_n^2 \right) P_n \right] \mod 1, \tag{7}$$

which is close to the Newtonian standard map (eqs. (1) and (2)) since $\beta P \ll 1$ in eq. (7).

The mean square momentum displacement (MSMD) is defined [1–3,7,10,11] as

$$\left\langle (\Delta P_n)^2 \right\rangle \equiv \left\langle (P_n - P_0)^2 \right\rangle, \tag{8}$$

where $\langle \ldots \rangle$ is an average over an ensemble of trajectories. In our calculations, in addition to using an initially non-localized semi-uniform ensemble, we also use an initially localized ensemble where the initial positions and momentums are both Gaussian distributed

$$\rho(X, P, t=0) = \frac{1}{2\pi \sigma_{X_0} \sigma_{P_0}} \exp \left[-\frac{1}{2} \left[\left(\frac{X - \langle X_0 \rangle}{\sigma_{X_0}} \right)^2 + \left(\frac{P - \langle P_0 \rangle}{\sigma_{P_0}} \right)^2 \right] \right], \tag{9}$$

with means $\langle X_0 \rangle$ and $\langle P_0 \rangle$, and standard deviations σ_{X_0} and σ_{P_0}. In each theory, the MSMD is first calculated using 10^6 trajectories (each trajectory in the ensemble is time-evolved using the corresponding standard map (either Newtonian (eqs. (1) and (2)) or special relativistic (eqs. (3) and (4)))), where the degree of numerical accuracy is determined by comparing the 30-significant-figure calculation with the 35-significant-figure (quadruple precision) calculation. For example, if the former calculation yields $1.234\ldots$, and the latter yields $1.235\ldots$, the 10^6 calculation is accurate to 1.23 (3 significant figures). The MSMD is then recalculated using 10^7 trajectories with the same degree-of-accuracy determination. Finally, the degree of accuracy of the MSMD is determined by comparing the 10^6 calculation with the 10^7 calculation. For example, if the 10^6 calculation is accurate to 1.23 and the 10^7 calculation is accurate to 1.24, the MSMD is accurate to 1.2 (2 significant figures). The Newtonian and special-relativistic MSMD are only compared after the degree of numerical accuracy of each MSMD has been determined by varying the numerical precision and the size of the ensemble in the manner described above. This method, which is a generalization of the standard numerical method [25] of establishing the degree of accuracy of a single trajectory, ensures that any conclusion resulting from the comparison of the Newtonian and special-relativistic MSMD is not due to numerical artifacts.
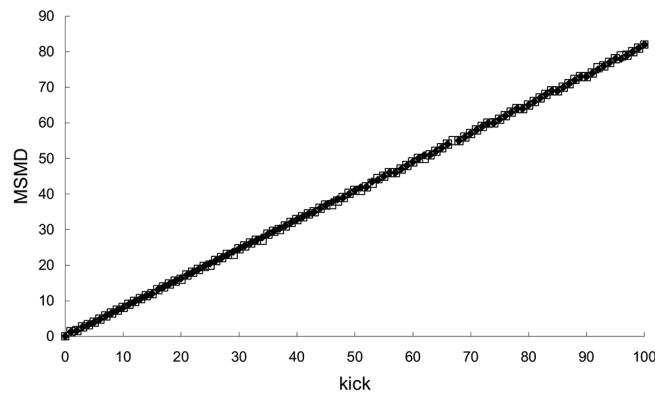
Fig. 1. Newtonian (squares) and special-relativistic (diamonds) MSMD in the first example where the initial ensemble is semi-uniformly distributed. MSMD which cannot be resolved in accuracy is not plotted.
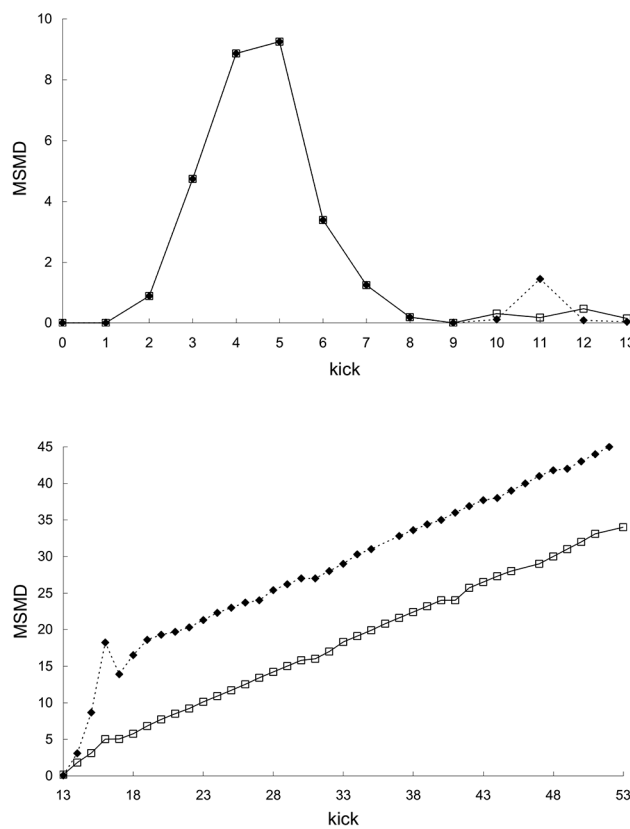
Fig. 2. Newtonian (squares) and special-relativistic (diamonds) MSMD in the second example for the first 13 kicks (top plot) and from kick 13 to kick 53 (bottom plot). MSMD which cannot be resolved in accuracy is not plotted.

Results

In this section, we will present three examples to illustrate the general results of comparing the low-speed MSMD predicted by Newtonian and special-relativistic mechanics for the kicked particle. In all the examples presented here, the parameter β in the relativistic standard map (eqs. (3) and (4)) is small, 10^{-7}, and so the mean particle speed is low [18], at most about 0.001% of the speed of light.

If the initial ensemble is semi-uniformly distributed, where the initial positions X_0 are uniformly distributed between 0 and 1 and all initial momenta are P_0, then there is generally no breakdown of agreement between the Newtonian and special-relativistic MSMD, which grow either linearly or as a power law from the outset. An example (this is our first example) is given in fig. 1 for $P_0 = 99.9$ and $K = 10.053$ (accelerator mode island does not [2] exist for this parameter), where the two MSMD grow linearly at close rates from the outset.
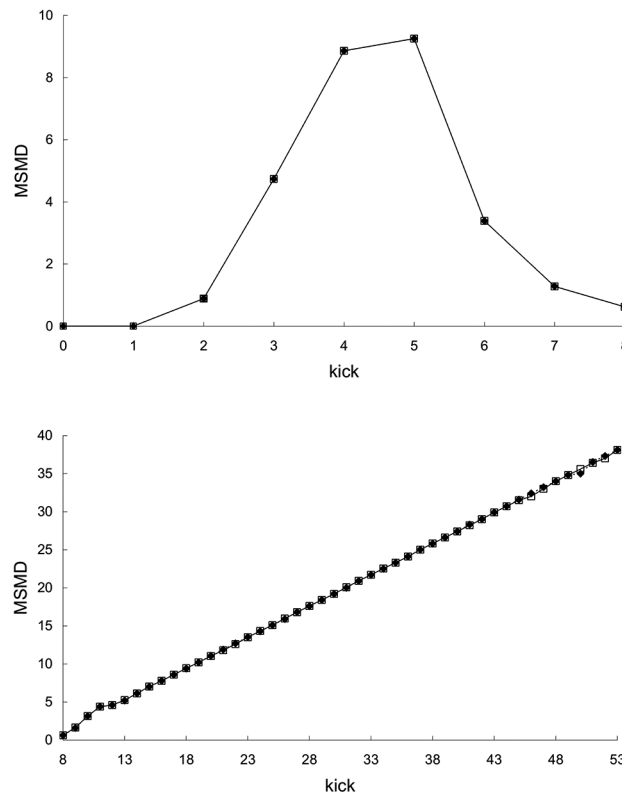
Fig. 3. Newtonian (squares) and special-relativistic (diamonds) MSMD in the third example for the first 8 kicks (top plot) and from kick 8 to kick 53 (bottom plot).

In the second example, the parameter K is also 10.053, but the ensemble is initially Gaussian localized in phase space with means $\langle X_0 \rangle = 0.5$ and $\langle P_0 \rangle = 99.9$, and standard deviations $\sigma_{X_0} = \sigma_{P_0} = 10^{-12}$. Figure 2 shows that the Newtonian and special-relativistic predictions for the MSMD are very close and fluctuating for the first 10 kicks, but, from kick 11 onwards, the MSMD predicted by the two theories disagree with each other completely. For example, at kick 11, the Newtonian and special-relativistic MSMD are, respectively, 0.173781 (accurate to 6 significant figures) and 1.443340 (accurate to 7 significant figures), where the degree of numerical accuracies were determined using the method described in the previous section.

In the third example, the parameter K and the means of the initial Gaussian ensemble are the same as those in the second example but the initial Gaussian ensemble is broader in both position and momentum with $\sigma_{X_0} = \sigma_{P_0} = 10^{-7}$. In contrast to the result in the second example, fig. 3 shows that there is no breakdown of agreement between the Newtonian and special-relativistic MSMD in this case.

The difference between the results for the second and third examples can be understood as follows. The Newtonian and special-relativistic position probability densities of the initially localized Gaussian ensemble are, as shown in [26], generally delocalized in the entire position interval from 0 to 1 when the position standard deviation reaches a saturation value of about $1/\sqrt{12} = 0.289$, which is the standard deviation of a uniform position density in the interval 0 to 1. In the second example, the Newtonian and special-relativistic position probability densities are delocalized at kick 13 and kick 15, respectively. In the third example, the position probability densities are both delocalized earlier, at kick 8. In each theory, before the delocalization of the position probability density, the MSMD,

$$\left\langle (P_n - P_0)^2 \right\rangle \equiv \sigma_{P_n}^2 + \langle P_n \rangle^2 - 2 \langle P_n P_0 \rangle + \sigma_{P_0}^2 + \langle P_0 \rangle^2 , \tag{10}$$

is dominated by

$$\langle P_n \rangle^2 - 2 \langle P_n P_0 \rangle + \langle P_0 \rangle^2 ,$$

which is approximately

$$\langle P_n \rangle^2 - 2 \langle P_n \rangle \langle P_0 \rangle + \langle P_0 \rangle^2 ,$$

since $\langle P_n P_0 \rangle \approx \langle P_n \rangle \langle P_0 \rangle$. Moreover, the mean trajectory $(\langle X_n \rangle, \langle P_n \rangle)$ of the ensemble is well approximated by the central trajectory (X_n, P_n), that is, the single trajectory with the same initial conditions as the mean trajectory:
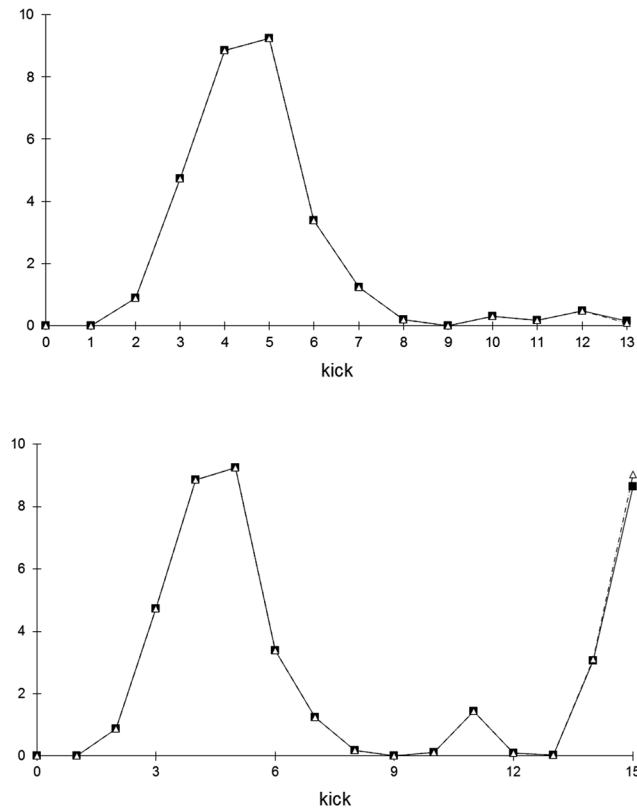
Fig. 4. Newtonian (top plot) and special-relativistic (bottom plot) MSMD (squares) and central-trajectory square momentum displacements (triangles) in the second example from zero kick until each ensemble is delocalized.

$X_0 = \langle X_0 \rangle$ and $P_0 = \langle P_0 \rangle$. Hence, the MSMD in each theory is approximately given by the square momentum displacement,

$$(P_n - P_0)^2 = P_n^2 - 2P_nP_0 + P_0^2, \tag{11}$$

of the central trajectory —see figs. 4 and 5 for, respectively, the second and third examples— before the position probability density is delocalized. In the second example, the breakdown of agreement between the Newtonian and special-relativistic MSMD at kick 11 (see fig. 2), before the delocalization of the position probability densities, is thus due to the breakdown of agreement between the Newtonian and special-relativistic central-trajectory square momentum displacements at kick 11, which is triggered by the breakdown of agreement between the Newtonian and special-relativistic central trajectories at kick 10. The breakdown of agreement between the central trajectories is not due to sensitivity to system parameter or initial conditions of the central trajectories since they are exactly the same in both theories; instead, it is due to the small difference involving v/c between the Newtonian map (eqs. (1) and (2)) and the special-relativistic map at low speed (see eqs. (6) and (7)). In contrast, in the third example, there is no breakdown of agreement between the Newtonian and special-relativistic MSMD because there is no breakdown of agreement between the Newtonian and special-relativistic central trajectories (the two central trajectories are the same as those in the second example where the breakdown occurs at kick 10) to trigger it before the position probability densities are delocalized at kick 8.

The second and third examples illustrate that the agreement between the Newtonian and special-relativistic MSMD breaks down after some time if the initial Gaussian ensemble is sufficiently localized in phase space such that the Newtonian and special-relativistic position probability densities are delocalized *after* the breakdown of agreement between the Newtonian and special-relativistic central trajectories. The breakdown of agreement between the two MSMD is triggered by the breakdown of agreement between the two central trajectories and occurs one kick after the agreement between the two central trajectories breaks down. The MSMD breakdown of agreement therefore occurs rapidly if the two central trajectories are chaotic, as the second example shows, but it would take a long time to occur if the two central trajectories are non-chaotic because the difference between the two trajectories only grows, on average, linearly, instead of exponentially [24].
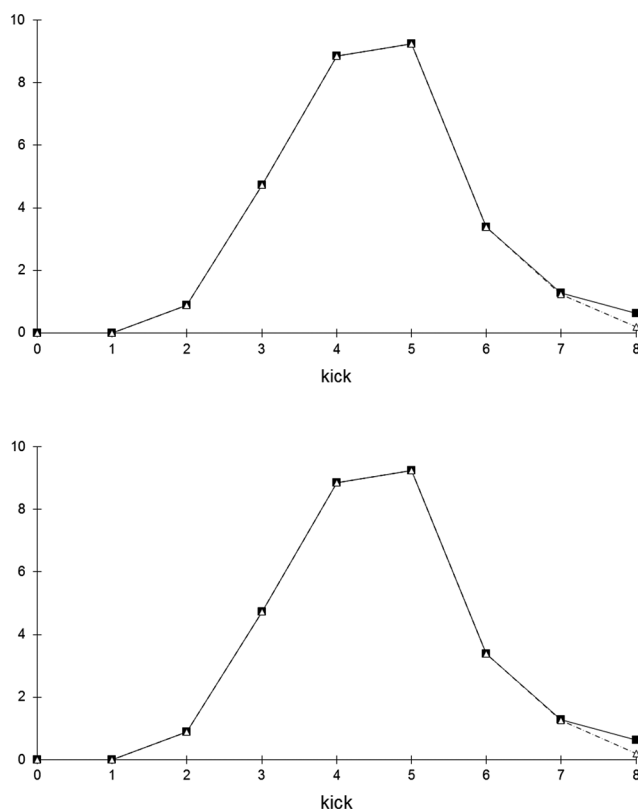
Fig. 5. Newtonian (top plot) and special-relativistic (bottom plot) MSMD (squares) and central-trajectory square momentum displacements (triangles) in the third example from zero kick until each ensemble is delocalized.

In each theory, after the position probability density is delocalized, the behavior of the MSMD calculated using an initially Gaussian ensemble is generally similar to the behavior of the MSMD calculated using an initially semi-uniform ensemble for the same parameter K, which is either linear growth or power-law growth. The linear growth rates or power-law exponents of the former MSMD (based on the initially localized ensemble) and latter MSMD (based on the initially non-localized ensemble) are close. In the second and third examples where $K = 10.053$, the growth is linear (see the bottom plots in figs. 2 and 3). In the second example, although the Newtonian and special-relativistic MSMD both grow linearly at close rates after the delocalization of the position probability densities, they start at different values and therefore the two MSMD remain different from one another (see the bottom plot in fig. 2). On the other hand, in the third example, the two MSMD remain close after the delocalization of the position probability densities because they grow linearly at close rates from close values (see the bottom plot in fig. 3).

Conclusion

In summary, there is no breakdown of agreement between the Newtonian and special-relativistic MSMD at low speed if the two MSMD are calculated using an initially non-localized semi-uniform ensemble. However, if an initially sufficiently localized Gaussian ensemble is used instead for calculations, the agreement between the two MSMD breaks down after some time due to, essentially, the small difference between the Newtonian and special-relativistic maps at low speed. Since the small difference between the Newtonian and special-relativistic equations of motion at low speed is generic, we expect similar breakdown of agreement between the Newtonian and special-relativistic predictions for low-speed momentum diffusion to occur in other nonlinear Hamiltonian systems. Therefore it should not be assumed that the Newtonian calculations will always yield approximately the same results as special-relativistic mechanics.

References

 1. B.V. Chirikov, Phys. Rep. **52**, 263 (1979).
 2. R. Ishizaki, T. Horita, T. Kobayashi, H. Mori, Prog. Theor. Phys. **85**, 1013 (1991).
 3. Y. Zheng, D.H. Kobe, Chaos Solitons Fractals **28**, 395 (2006).
 4. R. Ishizaki, H. Mori, Prog. Theor. Phys. **97**, 201 (1997).
 5. R. Ishizaki, H. Mori, Prog. Theor. Phys. **100**, 1131 (1998).
 6. G.M. Zaslavsky, M. Edelman, B.A. Niyazov, Chaos **7**, 159 (1997).
 7. A.A. Chernikov, B.A. Petrovichev, A.V. Rogal'sky, R.Z. Sagdeev, G.M. Zaslavsky, Phys. Lett. A **144**, 127 (1990).
 8. V.V. Afanasiev, R.Z. Sagdeev, G.M. Zaslavsky, Chaos **1**, 143 (1991).
 9. D.K. Chaikovsky, G.M. Zaslavsky, Chaos **1**, 463 (1991).
10. P. Lebœuf, Physica D **116**, 8 (1998).
11. R. Ishizaki, T. Horita, H. Mori, Prog. Theor. Phys. **89**, 947 (1993).
12. C.F.F. Karney, Physica D **8**, 360 (1983).
13. C.F.F. Karney, A.B. Rechester, R.B. White, Physica D **4**, 425 (1982).
14. J.D. Meiss, J.R. Cary, C. Grebogi, J.D. Crawford, A.N. Kaufman, H.D.I. Abarbanel, Physica D **6**, 375 (1983).
15. E.G. Altmann, H. Kantz, in *Anomalous Transport: Foundations and Applications*, edited by R. Klages, G. Radons, I.M. Sokolov (Wiley-VCH, Weinheim, 2008) pp. 269–292.
16. G.M. Zaslavsky, Phys. Rep. **371**, 461 (2002).
17. D.U. Matrasulov, G.M. Milibaeva, U.R. Salomov, B. Sundaram, Phys. Rev. E **72**, 016213 (2005).
18. A.P. French, *Special relativity* (Thomas Nelson & Sons, London, 1968) p. 167.
19. A. Einstein, *Relativity: the Special and the General Theory* (Random House, New York, 1961) pp. 49–50.
20. G. Casati, B.V. Chirikov, F.M. Izrailev, J. Ford, in *Stochastic Behavior in Classical and Quantum Hamiltonian Systems*, edited by G. Casati, J. Ford (Springer, 1979) pp. 334–351.
21. J.M. Greene, J. Math. Phys. **20**, 1183 (1979).
22. A.A. Chernikov, T. Tél, G. Vattay, G.M. Zaslavsky, Phys. Rev. A **40**, 4072 (1989).
23. Y. Nomura, Y.H. Ichikawa, W. Horton, Phys. Rev. A **45**, 1103 (1992).
24. B.L. Lan, Chaos **16**, 033107 (2006).
25. A.J. Lichtenberg, M.A. Lieberman, *Regular and stochastic motion* (Springer, New York, 1983) pp. 213–308.
26. S.N. Liang, B.L. Lan, PLOS **ONE 7**, e36430 (2012).